

# Nanomechanical Detection of DNA Melting on Microcantilever Surfaces

Sibani Lisa Biswal,<sup>†</sup> Digvijay Raorane,<sup>†</sup> Alison Chaiken,<sup>‡</sup> Henryk Birecki,<sup>‡</sup> and Arun Majumdar<sup>\*†</sup>

Department of Mechanical Engineering, UC Berkeley, Berkeley, California 94720, and HP Labs, Palo Alto, California 94306

We observe surface stress changes in response to thermal dehybridization, or melting, of double-stranded DNA (dsDNA) oligonucleotides that are grafted on one side of a microcantilever beam. Changes in surface stress occur when one complementary DNA strand melts and diffuses away from the other, resulting in alterations of the electrostatic, counterionic, and hydration interaction forces between the remaining neighboring surface-grafted DNA molecules. We have been able to distinguish changes in the melting temperature of dsDNA as a function of salt concentration and oligomer length. This technique also highlights differences between surface immobilized and solution DNA melting dynamics, which allows us to better understand the stability of DNA on surfaces. The transduction of phase transitions into a mechanical signal is ubiquitous for DNA, making cantilever-based detection a widely useful and complementary alternative to calorimetric and fluorescence measurements.

Configuration and conformational changes in biomolecules, including phase transitions, play a critical role in many biological processes. Given that they are driven by free energy reductions that usually involve enthalpy changes, they are often detected by calorimetric measurements.<sup>1</sup> Differential scanning calorimetry has shown to effectively measure the melting temperature ( $T_m$ ) and enthalpy of homogeneous and heterogeneous DNA strands.<sup>2</sup> Despite the fact that enthalpy microarrays<sup>3</sup> have been developed for multiplexed calorimetry, thermal insulation of a calorimeter from its surroundings becomes increasingly difficult for small samples where the surface-to-volume ratio increases.

Calorimetry is also used as a label-free technique to study specific biomolecular binding reactions and has been widely employed in applications such as drug discovery.<sup>4,5</sup> The detection of specific biomolecular interactions in complex mixtures is also

very important for disease diagnosis, genomics, and proteomics research. Most current approaches that use ligand–receptor binding, such as DNA microarrays and enzyme-linked immunosorbent assays, rely on the labeling of samples with a fluorescent or radioactive tag.<sup>6,7</sup> For small molecules, the tag could significantly change the chemistry or structure of the molecule itself, thereby motivating label-free approaches. Label-free methods include the surface plasmon resonance<sup>8</sup> and mass-based detection using a quartz crystal microbalance.<sup>9,10</sup> Most recently, microcantilever sensors have been shown to detect surface stress changes upon specific ligand–receptor binding, and thereby forming a new way for label-free detection.<sup>11–16</sup> What has remained elusive is whether such sensors can be used to study phase transitions or conformational changes such as those observed by calorimetry. In this paper, we use surface-grafted DNA as a model system to demonstrate that it is indeed possible.

The increasing number of applications for surface-grafted DNA has spurred a surge of activity aimed at increasing the understanding of the properties of DNA as a thin film. Of particular interest is the analysis of the melting temperature of DNA bound to surfaces. In this configuration, DNA has physical properties different from those of the bulk material due to interfacial interactions and effects of molecular confinement.<sup>17–22</sup> Many groups have used surface-bound DNA analysis to detect single-

\* Corresponding author. E-mail: majumdar@me.berkeley.edu.

<sup>†</sup> UC Berkeley.

<sup>‡</sup> HP Labs.

- Cooper, A.; Johnson, C. M.; Lakey, J. H.; Nollmann, M. *Biophys. Chem.* **2001**, *93*, 215–230.
- Riccelli, P. V.; Hall, T. S.; Pancoska, P.; Mandell, K. E.; Benight, A. S. *J. Am. Chem. Soc.* **2003**, *125*, 141–150.
- Torres, F. E.; Kuhnt, P.; De Bruyker, D.; Bell, A. G.; Wolkin, M. V.; Peeters, E.; Williamson, J. R.; Anderson, G. B.; Schmitz, G. P.; Recht, M. I.; Schweizer, S.; Scott, L. G.; Ho, J. H.; Elrod, S. A.; Schultz, P. G.; Lerner, R. A.; Bruce, R. H. *Proc. Natl. Acad. Sci. U. S. A.* **2004**, *101*, 9517–9522.
- Cooper, M. A. *Anal. Bioanal. Chem.* **2003**, *377*, 834–842.
- Perozzo, R.; Folkers, G.; Scapozza, L. *J. Recept. Signal Transduction* **2004**, *24*, 1–52.

- Mansfield, E. S.; Worley, J. M.; McKenzie, S. E.; Surrey, S.; Rappaport, E.; Fortina, P. *Mol. Cell. Probes* **1995**, *9*, 145–156.
- Stimpson, D. I.; Hoijer, J. V.; Hsieh, W. T.; Jou, C.; Gordon, J.; Theriault, T.; Gamble, R.; Baldeschwieler, J. D. *Proc. Natl. Acad. Sci. U. S. A.* **1995**, *92*, 6379–6383.
- Homola, J.; Yee, S. S.; Gauglitz, G. *Sens. Actuators, B* **1999**, *54*, 3–15.
- Babacan, S.; Pivarnik, P.; Letcher, S.; Rand, A. G. *Biosens. Bioelectron.* **2000**, *15*, 615–621.
- Bailey, L. E.; Kambhampati, D.; Kanazawa, K. K.; Knoll, W.; Frank, C. W. *Langmuir* **2002**, *18*, 479–489.
- Hansen, K. M.; Ji, H. F.; Wu, G. H.; Datar, R.; Cote, R.; Majumdar, A.; Thundat, T. *Anal. Chem.* **2001**, *73*, 1567–1571.
- Wu, G. H.; Ji, H. F.; Hansen, K.; Thundat, T.; Datar, R.; Cote, R.; Hagan, M. F.; Chakraborty, A. K.; Majumdar, A. *Proc. Natl. Acad. Sci. U. S. A.* **2001**, *98*, 1560–1564.
- Yue, M.; Lin, H.; Dedrick, D. E.; Satyanarayana, S.; Majumdar, A.; Bedekar, A. S.; Jenkins, J. W.; Sundaram, S. *J. Microelectromech. Syst.* **2004**, *13*, 290–299.
- Tian, F.; Hansen, K. M.; Ferrell, T. L.; Thundat, T. *Anal. Chem.* **2005**, *77*, 1601–1606.
- Thundat, T.; Majumdar, A. In *Sensors and Sensing in Biology and Engineering*; Springer-Verlag: New York, 2003.
- Marie, R.; Jensenius, H.; Thaysen, J.; Christensen, C. B.; Boisen, A. *Ultramicroscopy* **2002**, *91*, 29.
- Peterlinz, K. A.; Georgiadis, R. M.; Herne, T. M.; Tarlov, M. *J. Am. Chem. Soc.* **1997**, *119*, 3401–3402.
- Peterson, A. W.; Heaton, R. J.; Georgiadis, R. *J. Am. Chem. Soc.* **2000**, *122*, 7837–7838.

64 nucleotide polymorphisms (SNPs) for genomic information.<sup>23,24</sup>  
 65 Dynamic allele-specific hybridization is a novel SNP detecting  
 66 method based on allele-specific hybridization followed by dynamic  
 67 heating and simultaneous monitoring of the denaturation profile  
 68 using fluorescently labeled probes or intercalating dyes.<sup>25</sup> The  
 69 melting temperature of the sequence containing a SNP is lower  
 70 than fully hybridized strands. One recent paper has reported  
 71 combining molecular beacons with microfluidics to study the  
 72 thermal dehybridization of surface-bound DNA.<sup>26</sup> Other studies  
 73 using gold nanoparticles have shown sharper and higher melting  
 74 transitions when using a nanoparticle–DNA aggregate or a  
 75 nanoparticle/complementary strand/surface-bound DNA complex  
 76 compared to conventional fluorophore probe studies.<sup>27,28</sup>

77 We propose using microcantilever sensors to detect DNA  
 78 melting by heating the microcantilevers while monitoring the  
 79 cantilever deflection. When biomolecules are immobilized onto  
 80 one surface of the cantilever, changes in the surface stress on  
 81 that side of the cantilever induce bending. Stoney's formula relates  
 82 the change in surface stress to the change in cantilever deflection:  
 83<sup>29</sup>

$$\Delta h = \frac{3\Delta\gamma(1 - \nu_1)L^2}{E_1 t_1^2} \quad (1)$$

84 where  $\Delta\gamma$  is the change in surface stress,  $\nu_1$  is Poisson's ratio for  
 85 the thick layer,  $E_1$  is Young's modulus for the thick layer,  $t_1$  is  
 86 the thickness of the thick layer,  $L$  is the length of the cantilever,  
 87 and  $\Delta h$  is the deflection of the cantilever. The advantage of  
 88 microcantilevers is that they allow detection of phase transitions  
 89 in the steady state without the use of a labeling probes or costly  
 90 reagents. We use this concept of surface stress change to monitor  
 91 the melting of surface immobilized DNA. As the temperature of  
 92 the cantilever is raised, there is a conformational change of the  
 93 DNA molecules as it undergoes a transition from double- to single-  
 94 stranded, resulting in a change in the surface stress of the layer.  
 95 The cantilever either shrinks due to tensile stress or expands due  
 96 to compressive stress. Berger et al. has demonstrated a similar  
 97 detection of phase transitions using alkanethiols.<sup>30</sup> In this paper,  
 98 we have utilized the thermally induced bending phenomenon to  
 99 study phase transitions in DNA films on microcantilevers for  
 100 varying DNA lengths and solution ionic strengths.

- (19) Peterson, A. W.; Heaton, R. J.; Georgiadis, R. M. *Nucleic Acids Res.* **2001**, *29*, 5163–5168.  
 (20) Peterson, A. W.; Wolf, L. K.; Georgiadis, R. M. *J. Am. Chem. Soc.* **2002**, *124*, 14601–14607.  
 (21) Petrovykh, D. Y.; Kimura-Suda, H.; Whitman, L. J.; Tarlov, M. J. *J. Am. Chem. Soc.* **2003**, *125*, 5219–5226.  
 (22) Meunier-Prest, R.; Raveau, S.; Finot, E.; Legay, G.; Cherkaoui-Malki, M.; Latruffe, N. *Nucleic Acids Res.* **2003**, *31*.  
 (23) Mao, H. B.; Holden, M. A.; You, M.; Cremer, P. S. *Anal. Chem.* **2002**, *74*, 5071–5075.  
 (24) Mukhopadhyay, R.; Lorentzen, M.; Kjems, J.; Besenbacher, F. *Langmuir* **2005**, *21*, 8400–8408.  
 (25) Prince, J. A.; Feuk, L.; Howell, W. M.; Jobs, M.; Emahazion, T.; Blennow, K.; Brookes, A. J. *Genome Res.* **2001**, *11*, 152–162.  
 (26) Dodge, A.; Turcatti, G.; Lawrence, I.; de Rooij, N. F.; Verpoorte, E. *Anal. Chem.* **2004**, *76*, 1778–1787.  
 (27) Jin, R. C.; Wu, G. S.; Li, Z.; Mirkin, C. A.; Schatz, G. C. *J. Am. Chem. Soc.* **2003**, *125*, 1643–1654.  
 (28) Taton, T. A.; Mirkin, C. A.; Letsinger, R. L. *Science* **2000**, *289*, 1757–1760.  
 (29) Stoney, G. G. *Proc. R. Soc. London, Ser. A* **1909**, *82*, 172–175.  
 (30) Berger, R.; Gerber, C.; Gimzewski, J. K.; Meyer, E.; Guntherodt, H. J. *Appl. Phys. Lett.* **1996**, *69*, 40–42.

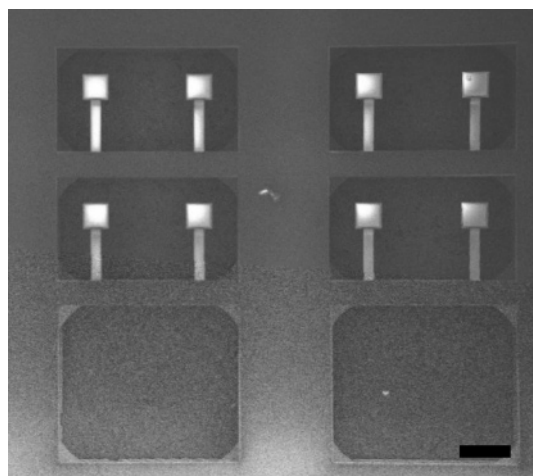


**Figure 1.** SEM picture of microcantilever array chip used in melting experiments. Scale bar, 200  $\mu\text{m}$ .

Denaturation of DNA is induced by using heat or chemical  
 treatments to separate the double helix into two single strands.  
 This process is often thought to be cooperative so that the AT-  
 rich regions melt first, destabilizing the neighboring helical  
 structure. The separated strands can either rehybridize or undergo  
 a coil-to-globule transition in solution.<sup>31</sup> The melting temperature,  
 $T_m$ , of bulk DNA in solution is well determined by spectroscopy,  
 and many empirical formulas have been developed to account for  
 both the ionic strength and the mole fraction of G–C base pairs.<sup>32</sup>  
 However, the environment of oligomers can differ between a solid  
 interface and the bulk solution due to difference between ionic  
 strengths. We use the cantilevers to highlight the differences  
 between  $T_m$  in solution and on a solid support.

## MATERIALS AND METHODS

**Microcantilever Array.** Preparation of the microcantilever  
 array has been described previously.<sup>13</sup> A low-pressure chemical  
 vapor deposition of low-stress silicon nitride and thermal evapora-  
 tion of chromium and gold layers is performed on a silicon wafer.  
 Each cantilever sensor consists of a released silicon nitride beam  
 that is 500 nm thick, 40  $\mu\text{m}$  wide, and 200  $\mu\text{m}$  long. A rigid paddle  
 structure is fabricated at the end of the beam to provide a flat  
 surface that assists with the optical detection of the beam's  
 reflection. On one side of the beam, there is a 5-nm chromium  
 layer, which is used to facilitate the adhesion of a 25-nm-thick  
 gold layer. The gold layer provides a reflective surface as well as  
 an interface for attaching functional probe molecules. A Pyrex  
 wafer containing wet-etched microfluidic chambers is bonded to  
 the chip using a UV curing adhesive (Norland 121). The 2-cm<sup>2</sup>  
 cantilever chip shown in Figure 1 is made up of a 15  $\times$  6 array of  
 individual fluid chambers, each of which contains four cantilevers.  
 We average the responses of the four cantilevers to increase the  
 accuracy of the measurements.

To image the cantilever array, a helium–neon laser (632.8 nm,  
 15 mW) is expanded to illuminate the entire chip as it sits in a  
 temperature-controlled holder. All reflections pass through a beam  
 splitter, which directs half the reflected intensity from the

- (31) Marky, L. A.; Kallenbach, N. R.; McDonough, K. A.; Seeman, N. C.;  
 Breslauer, K. J. *Biopolymers* **1987**, *26*, 1621–1634.  
 (32) Blake, R. D.; Delcourt, S. G. *Nucleic Acids Res.* **1998**, *26*, 3323–3332.

**Table 1. DNA Sequences Used and Corresponding Calculated Using OligoAnalyzer 3.0 in SciTools (<http://www.idtdna.com/>)**

| name    | sequence                              | $T_{m, \text{calculated}}$ ( $^{\circ}\text{C}$ ) |                        |                         |
|---------|---------------------------------------|---|------------------------|-------------------------|
|         |                                       | 25 mM $\text{Na}^+$                               | at 50 mM $\text{Na}^+$ | at 100 mM $\text{Na}^+$ |
| ls15    | 5'-thiol-CTACTAAATACAAAT-3'           | 24.7  | 30.6                   | 35.8                    |
| comp15  | 5'-ATTTGTATTTAGTAG-3'                 |   |                        |                         |
| ls20    | 5'-thiol-TTTTTTTTATTCAATTTATT-3'      | 30.2  | 36.7                   | 42.1                    |
| comp20  | 5'-AATAAATTGAATAAAAAAAA-3'            |   |                        |                         |
| ls25    | 5'-thiol-TTTTTTTTATTCATTTTACTTTTTT-3' | 37.1  | 43.8                   | 49.9                    |
| comp25  | 5'-AAAAAAGTAAAATGAATAAAAAAAA A-3'     |   |                        |                         |
| ss20    | 5'-thiol- GTGGTAGATGAAGGTGAGAG -3'    | 46.1  | 51.9                   |                         |
| dcomp20 | 5'- CTCTCACCTTCATCTACCAC -3'          |   |                        |                         |

137 cantilever array onto a CCD camera chip (Apogee Inc.,  $3072 \times$   
 138  $2048$  pixels, 16 bit). The frame capture rate is 1 frame every 10 s.  
 139 Once aligned with the optical system, individual cantilever reflections  
 140 appear as spots in the CCD image. A Matlab particle tracking  
 141 program tracks each cantilever paddle image by calculating the  
 142 intensity centroid of the spot.

143 The mismatch between the thermal expansion of the silicon  
 144 nitride and the gold causes the well-known thermal biomorph  
 145 effect. For each experiment, the thermomechanical response of  
 146 each cantilever is simultaneously measured in units of CCD  
 147 pixels/ $^{\circ}\text{C}$ . This value is later used to normalize the cantilever  
 148 bending induced by biomolecular reactions. A white-light interferometer  
 149 (Veeco) is then used to measure the thermomechanical  
 150 response of the cantilevers (in nm/ $^{\circ}\text{C}$ ). As described previously,<sup>23</sup>  
 151 this interferometry provides the calibration (pixel/nm) between  
 152 motion of the laser spot on the CCD image and the absolute  
 153 cantilever deflection in nanometers. The deflection of the cantilevers  
 154 is then used to calculate the surface stress caused by  
 155 biomolecular reactions using Stoney's formula. The previously  
 156 measured thermomechanical sensitivity of the cantilevers is 208  
 157 nm/K with a standard deviation of 14 nm/K.<sup>13</sup> In terms of surface  
 158 stress, a 1 K change in temperature corresponds to a stress change  
 159 of 24.5 mJ/m<sup>2</sup>.

160 Before an experiment, a chip is cleaned in 2-propanol, rinsed  
 161 with deionized water, and equilibrated in phosphate buffer for at  
 162 least 15 min. Then the chip is mounted in the chip holder with a  
 163 temperature controller (model LCP-3215, Wavelength Electronics).  
 164 The temperature controller has a control band of  $\sim 10$  mK. The  
 165 temperature of the chip holder is monitored using a thermocouple  
 166 temperature recorder (VWR). The cantilever deflection due to a  
 167 temperature change of 1  $^{\circ}\text{C}$  is recorded to establish the thermo-  
 168 mechanical sensitivity of each cantilever. Using this measurement,  
 169 the movement of the spot reflection in response to a surface  
 170 reaction can be converted into a surface stress change.

171 **Oligonucleotide Immobilization.** To prevent nonspecific  
 172 binding to the silicon nitride side of the cantilever, a PEG-silane  
 173 coating is prepared. A solution of 100  $\mu\text{L}$  of 2-methoxy(polyethy-  
 174 lenoxy)propyltrimethoxysilane (Gelest Inc.) with 40  $\mu\text{L}$  of HCl  
 175 in 50 mL of toluene is sonicated for 15 min. The chip is incubated  
 176 in the solution overnight.

177 Four different capture single-stranded (ss) DNA probes and  
 178 their complementary (Integrated DNA Technologies (IDT), Cor-  
 179 alville, IL) strands were used for the measurements. As shown in  
 180 Table 1, the sequences differ in length and melting temperatures.  
 181 The ssDNA has a thiol group attached to the 5'-end through a

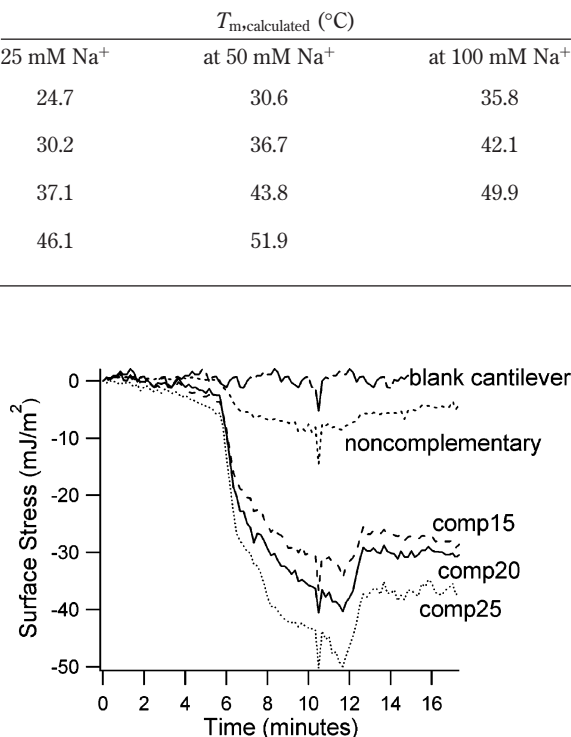


**Figure 2.** Hybridization results for three sets of DNA. We see that there is no surface stress change on the blank cantilever, a minimal amount when noncomplementary DNA is added, and a surface stress change in the range of 30–40 mJ/m<sup>2</sup> when complementary target DNA is added.

(CH<sub>2</sub>)<sub>6</sub> linker for covalent attachment to the gold surface of the  
 cantilever. DNA disulfide groups were reduced with 0.1 M  
 dithiothreitol (DTT), and the excess DTT was removed using a  
 NAP-10 column. The oligonucleotide attachment on the cantilever  
 was done by injecting each 1.5- $\mu\text{L}$  well with 1.0  $\mu\text{L}$  of 1  $\mu\text{M}$   
 thiolated ssDNA in 50 mM phosphate-buffered saline (PBS; pH  
 7.0). The chip was held at room temperature during the adsorption  
 experiments. The cantilever response was monitored for 1 h after  
 exposure to the ssDNA solution to confirm immobilization. The  
 chip was then left to incubate overnight with the solution.

**Hybridization/Dehybridization Experiments.** After immo-  
 bilization, each well is rinsed with a 50 mM PBS buffer several  
 times to remove unattached oligonucleotides. The wells were then  
 injected with the complementary sequence dissolved in a 50 mM  
 PBS buffer. As controls, plain buffer and a solution with a  
 noncomplementary sequence were injected into different wells.  
 Again, the chip was held at room temperature during the  
 hybridization experiments. The cantilever response was monitored  
 for  $\sim 1$  h to ensure successful hybridization had occurred. After  
 this time, the wells are washed with PBS buffer at the desired  
 ionic strength and covered with a poly(dimethylsiloxane) piece  
 to prevent evaporation of the solution from the wells.

Melting curves are acquired by slowly ramping up the  
 temperature to anywhere between 25 and 50  $^{\circ}\text{C}$  at a rate of  $\sim 1$   
 $^{\circ}\text{C}/\text{min}$  and simultaneously measuring the temperature using the



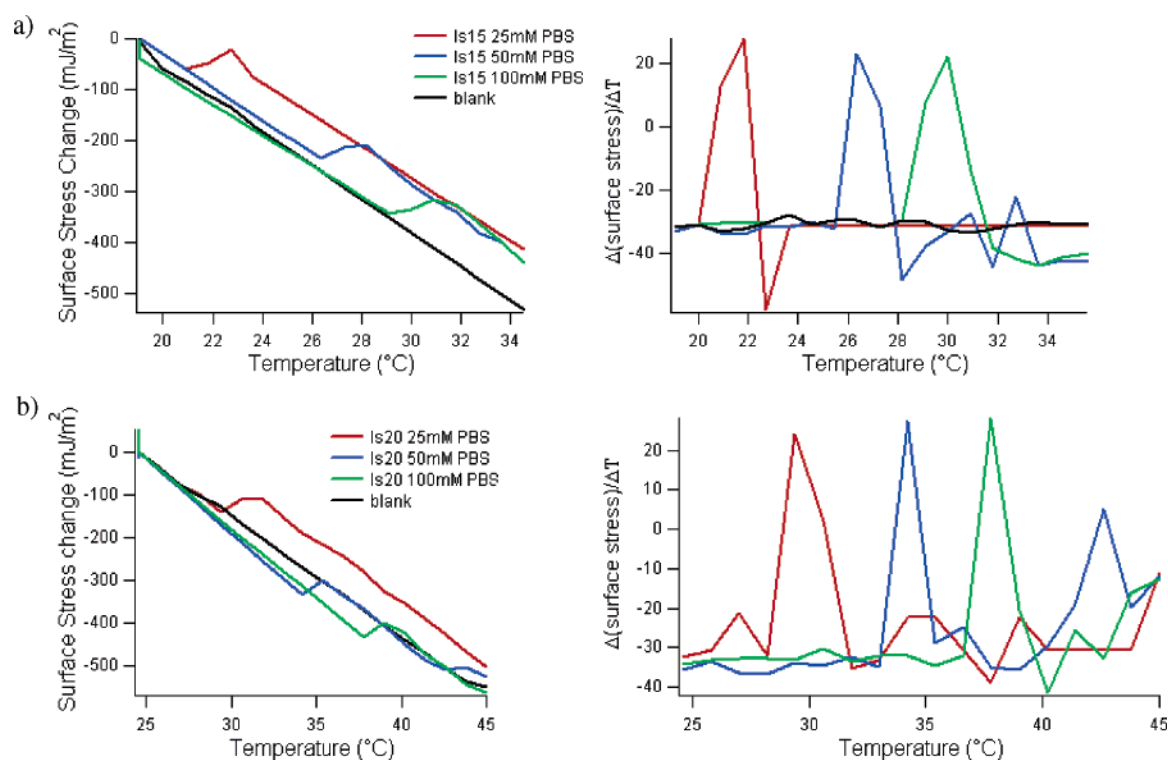


**Figure 3.** Surface stress vs temperature at various buffer salt concentrations and the derivative of the surface stress with respect to temperature are shown for (a) Is15 and (b) Is20. The melting temperature can be determined by the position of the peaks.

207 thermocouple recorder. The temperature range is limited to  $\sim 20$   
 208  $^{\circ}\text{C}$  in our optical system. Once the temperature change is greater  
 209 than  $20^{\circ}\text{C}$ , the spots become difficult to track because they fade  
 210 as they go out of focus. For this reason, we align the optics to  
 211 accommodate the desired temperature range. The total run time  
 212 is  $\sim 20$  min.

213 Repeated measurements were performed on the same im-  
 214 mobilized oligonucleotides. The wells were rinsed with PBS  
 215 buffer to remove the dehybridized DNA probes leaving the ssDNA  
 216 strands on the surface.

## 217 RESULTS AND DISCUSSION

218 **Immobilization/Hybridization Experiments.** As previously  
 219 shown, cantilever deflection results from an increase in surface  
 220 stress due to hybridization of DNA strands to complementary  
 221 DNA strands on the surface.<sup>13</sup> Cantilever deflection as a function  
 222 of time for the hybridization of target ssDNA to surface im-  
 223 mobilized probes is shown in Figure 2. The injection of the sample  
 224 occurs at  $t = 6$  min. The matching sequence hybridizes and  
 225 produces a change in surface stress of  $30\text{--}40\text{ mJ/m}^2$ , which in  
 226 turn leads to bending of the cantilever. The system is sensitive to  
 227 external disturbances as seen by the spike at  $t = 10$  min, but  
 228 stabilizes afterward. The small decrease in the signal at  $t = 12$   
 229 min is associated with desorption of loosely bound oligonucleo-  
 230 tides. Hybridization between the immobilized probe and the  
 231 matching target causes the cantilever to bend away from the gold  
 232 surface. To confirm that the deflection signals are caused by DNA  
 233 hybridization,  $5\ \mu\text{M}$  noncomplementary ssDNA is also injected  
 234 into a different well for comparison. As shown in Figure 2, injection  
 235 of noncomplementary ssDNA produces only a minimal deflection  
 236 produced after this injection, most likely due to nonspecific  
 237 interactions of the oligonucleotides with the functionalized mi-

crocantilever surfaces. The blank cantilevers in wells containing  
 238 only buffer do not bend when the target sequence is injected.  
 239 Therefore, those cantilevers serve as reference sensors.  
 240

241 Previously, it was observed that probe immobilization and  
 242 hybridization on microcantilevers depends on a variety of factors  
 243 such as probe length, probe surface density, and ionic strength  
 244 of solution.<sup>33,34</sup> The complex parameter dependence is due to the  
 245 interplay of forces, including short-range chemical interactions of  
 246 covalent gold/thiol attachment and long-range electrostatic repul-  
 247 sion and hydration forces between DNA strands. When consider-  
 248 ing ionic strengths, at low ionic strengths, fewer probes adsorb  
 249 because of the larger electrostatic repulsion between probe  
 250 strands. In high ionic strength solutions, the electrostatic repul-  
 251 sions between probe molecules are effectively screened, and  
 252 higher probe coverage can be reached limited only by hydration  
 253 interactions. The changes in film thickness due to hybridization  
 254 also affect the surface stress on the microcantilevers. When single  
 255 strands are immobilized, the strands are in a more coiled and  
 256 compact conformation. Upon introduction and subsequent hy-  
 257 bridization of complementary target DNA strands, the double-  
 258 stranded DNA takes on a rodlike conformation, which results in  
 259 an increase in the DNA film thickness.<sup>35</sup> We observe this increase  
 260 in film thickness as an increase in surface stress on the micro-  
 261 cantilevers surface. In our experiments, we kept both the im-  
 262 mobilization and hybridization conditions fixed at  $50\text{ mM}$  buffer  
 263 solution. Previous studies<sup>36</sup> have shown that these conditions

(33) Hagan, M. F.; Majumdar, A.; Chakraborty, A. K. *J. Phys. Chem. B* **2002**, *106*, 10163–10173.

(34) Hagan, M. F.; Chakraborty, A. K. *J. Chem. Phys.* **2004**, *120*, 4958–4968.

(35) Steel, A. B.; Levicky, R. L.; Herne, T. M.; Tarlov, M. *J. Biophys. J.* **2000**, *79*, 975–981.

(36) Castelino, K.; Kannan, B.; Majumdar, A. *Langmuir* **2005**, *21*, 1956–1961.

264 result in a grafting density of probe immobilization of 0.03–0.05  
265 probes/nm<sup>2</sup>.

266 **Melting Experiments.** We use the microcantilevers to measure  
267 the melting temperature,  $T_m$ , for each oligonucleotide in three  
268 different ionic strength solutions: 25, 50, and 100 mM. In the  
269 presence of buffer solution, the cantilever deflects away from the  
270 gold surface with increasing temperature due to the thermal  
271 biomorph effect. This effect is also seen with cantilevers bound  
272 with DNA. However, there are discontinuities in the melting profile  
273 at varying locations depending on the buffer salt concentration.  
274 We associate these discontinuities with phase transitions in the  
275 surface-bound DNA films. As shown in Figure 3, the deflection  
276 data for a blank cantilever, which has been normalized by its  
277 thermomechanical response and converted to surface stress  
278 versus temperature, display a characteristic linear response to  
279 temperature change. Also shown in Figure 3, cantilevers with DNA  
280 display sharp transitions in the surface stress data that deviate  
281 from a linear response. By plotting the derivative of the surface  
282 stress with respect to temperature ( $d\delta/dT$ ), we find the temper-  
283 ature at which the cantilever response deviates from linearity,  
284 which we attribute to DNA melting. The abrupt change in the  
285 cantilever deflection is characteristic of a two-state melting  
286 transition.<sup>37</sup> The melting temperature of untethered complexes is  
287 calculated using the following thermodynamic relationship:  $T_m$   
288 =  $\Delta H^\circ / (\Delta S^\circ + R \ln C_t)$ , where the changes in standard enthalpy  
289 ( $\Delta H$ ) and entropy ( $\Delta S$ ) associated with duplex formation are  
290 calculated using nearest-neighbor thermodynamic parameters,  $R$   
291 is the gas constant, and  $C_t$  is the concentration of the oligonucle-  
292 otide.<sup>38,39</sup> These thermodynamic parameters and  $T_m$  are calculated  
293 using OligoAnalyzer 3.0 in SciTools (<http://www.idtdna.com/>).  
294 The calculated melting temperatures are expected to be accurate  
295 within a range of 2 °C.

296 Figure 4a summarizes the results for different oligonucleotides  
297 at varying salt concentrations. As expected, increasing salt  
298 concentration results in an increase in the melting temperature.  
299 A similar trend is also observed for increasing oligonucleotide  
300 length due to a well-known increase in the stability of the duplexes  
301 at higher salt concentrations and greater oligonucleotide  
302 lengths.<sup>40–42</sup> If we compare the two 20-mer oligonucleotides,  
303 represented by the diamond and circles in Figure 4a, we find that  
304 ss20, which is the more GC-rich sequence, melts at a higher  
305 temperature than ls20, which is more AT-rich DNA sequence. This  
306 is due to the fact that GC base pairs have three hydrogen bonds,  
307 while AT base pairs have only two.<sup>39</sup>

308 In general, we observe that surface-bound complexes melt at  
309 lower temperatures than their bulk melting temperatures as shown  
310 in Figure 4b, in which the difference between  $T_{m, \text{calculated}}$  and  
311  $T_{m, \text{experimental}}$  has been plotted as a function of salt concentration  
312 for each of the oligonucleotides. We believe that this reduction  
313 in melting temperature of surface-bound DNA results from

(37) Klump, H. H. In *Studies in Modern Thermodynamics 8: Biochemical Thermodynamics*, 2 ed.; Jones, M. N., Ed.; Elsevier: Amsterdam, 1988; pp 100–144.

(38) Sugimoto, N.; Nakano, S.; Yoneyama, M.; Honda, K. *Nucleic Acids Res.* **1996**, *24*, 4501–4505.

(39) Owczarzy, R.; Vallone, P. M.; Gallo, F. J.; Paner, T. M.; Lane, M. J.; Benight, A. S. *Biopolymers* **1997**, *44*, 217–239.

(40) Tikhomirova, A.; Taulier, N.; Chalikian, T. V. *J. Am. Chem. Soc.* **2004**, *126*, 16387–16394.

(41) Rouzina, I.; Bloomfield, V. A. *Biophys. J.* **1999**, *77*, 3242–3251.

(42) Bond, J. P.; Anderson, C. F.; Record, M. T. *Biophys. J.* **1994**, *67*, 825–836.

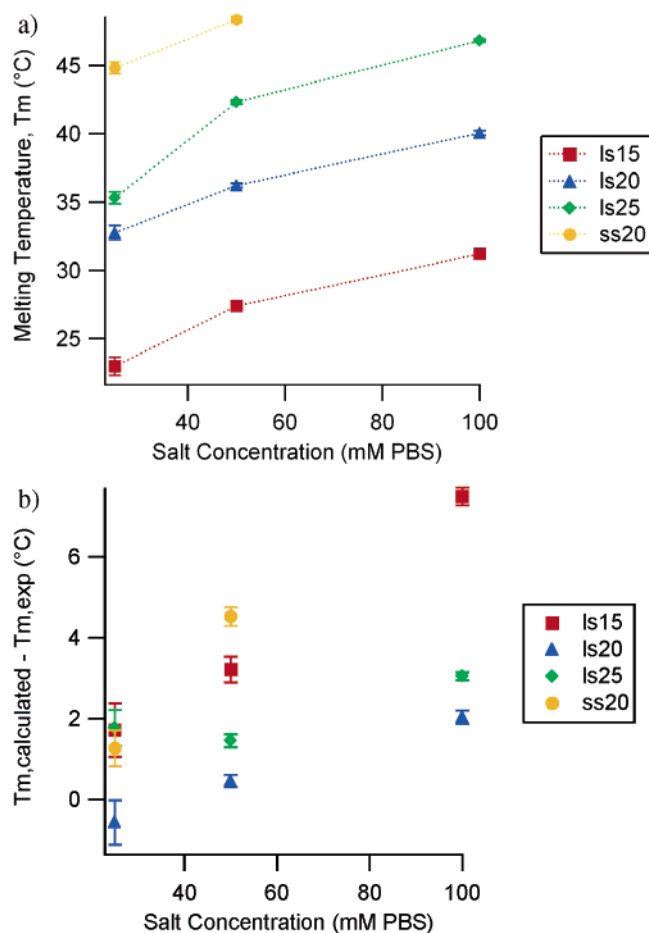


**Figure 4.** Summary of cantilever melting experiments given by salt concentration. (a) Average experimental melting temperature for each oligonucleotide at 25, 50, and 100 mM ionic strength solutions. (b) Difference between the calculated  $T_m$  and the experimental  $T_m$  for each oligonucleotide at 25, 50, and 100 mM ionic strength solutions. Error bars show standard deviation from 16 cantilever experiments.

314 duplexes being less stable on a surface compared to solution  
315 because of the difference between DNA dynamics in a bulk  
316 environment as compared to dynamics of DNA near an interface.  
317 Another interesting observation seen in Figure 4b is that the  
318 difference between  $T_{m, \text{calculated}}$  and  $T_{m, \text{experimental}}$  becomes more  
319 pronounced at higher ionic strengths, which has also been  
320 previously reported by Peterlinz et al.<sup>17</sup> We suspect that the  
321 enhancement of this destabilization on a surface is likely caused  
322 by two effects: the interactions of the strands with the surface  
323 and the interactions between neighboring strands. When consid-  
324 ering the effect of the surface, the main difference is that access  
325 to the immobilized oligomer for hybridization is sterically re-  
326 stricted due to its attachment to the surface. Confining DNA to  
327 the surface involves both energetic and entropic effects, with the  
328 balance between the two trends controlled by the stiffness of the  
329 chain and the length scale of confinement.<sup>40</sup> In the bulk solution,  
330 interactions between neighboring strands are oftentimes negligible  
331 and the denaturation events are considered independent of each  
332 other. However, on a surface, there are interactions between  
333 neighboring oligonucleotide strands that must be taken into  
334 account. To consider the effects of neighboring strands, we must  
335 consider the packing density of probes on the cantilever. For our  
336 experiments, the surface coverage is  $\sim 0.03$  probes/nm<sup>2</sup>. So the

337 area occupied by each strand is  $\sim 33 \text{ nm}^2$ , with an effective radius  
338 of 3.3 nm. Podgornik et al.<sup>43,44</sup> showed that arrays of DNA have  
339 strong repulsions between neighbors as the intermolecular  
340 distance is reduced below 3.2 nm. It is apparent that the  
341 thermodynamic stability of the DNA complex is dependent on  
342 nearest-neighbor interactions from ssDNA and nearby dsDNA.  
343 We are currently investigating the interactions between neigh-  
344 boring strands by probing the effects of surface coverage. When the  
345 temperature is reduced back to room temperature, we do not  
346 observe the rehybridization signal on the cantilever although we  
347 have performed successful melting scans after a 24-h wait for  
348 rehybridization. We believe that the lack of rehybridization is due  
349 to the diffusion of the melted oligonucleotides into the bulk solution.

## 350 CONCLUSION

351 We demonstrate that changes in surface stress in a microcan-  
352 tilever beam can be used to detect melting of surface-grafted DNA.  
353 Melting causes ones of the strands to dehybridize and diffuse away  
354 from the cantilever surface, leaving the surface with only single-

---

(43) Strey, H. H.; Parsegian, V. A.; Podgornik, R. *Phys. Rev. Lett.* **1997**, *78*, 895–898.

(44) Strey, H. H.; Podgornik, R.; Rau, D. C.; Parsegian, V. A. *Curr. Opin. Struct. Biol.* **1998**, *8*, 309–313.

stranded DNA, thereby modifying the force interaction between 355  
neighboring strands. Melting temperature decreases with chain 356  
length and salt concentration and is lower for surface-grafted DNA 357  
than for DNA in solution. 358

The purpose of using DNA in this project was to demonstrate 359  
the concept of utilizing the cantilever surface stresses for studying 360  
phase transitions. We feel, however, that the method will be 361  
applicable to the study of phase transitions in other biomolecules 362  
as well and more generally for study molecular configurational 363  
and conformational changes in any surface-grafted biomolecular 364  
systems. Such a label-free approach could be potentially very 365  
valuable in a variety of applications such as quantifying enzymatic 366  
activity and measuring the kinetics of ligand–receptor binding. 367

## ACKNOWLEDGMENT 368

This work is supported by the Center for Information Technol- 369  
ogy Research in the Interest of Society (CITRIS) through a grant 370  
provided by HP Labs. 371

Received for review December 8, 2005. Accepted May 15, 372  
2006. 373

AC052171Y 374